

# Position Sensitive Gas Proportional Detectors with Anode Blades<sup>1</sup>

B. Yu, G.C. Smith, D.P. Siddons, P.J. Pietraski and Z. Zojceski  
Brookhaven National Laboratory, Upton, NY 11973, USA

## Abstract

The use of a thin metal blade to generate controlled electron multiplication in gas proportional mode has been studied. Measurements with x-rays have been made on assemblies of an anode blade and two adjacent cathodes in a test chamber. Systematic studies of various detector parameters and their influences on the multiplication process have been carried out. Devices constructed using this technique are very rugged and can be tailored to a curved geometry for the purposes of eliminating parallax error for small and large angle x-ray scattering experiments. Experimental results of a curved, one-dimensional position sensitive detector for synchrotron radiation, with an arc length of 20cm and a 45° coverage, will be discussed.

## I. INTRODUCTION

The intense photon beams from second and, particularly, third generation synchrotron sources require the utmost performance from position sensitive detectors in terms of position resolution, count rate and stability. As an outgrowth of investigations on microstrip gas chambers, our group has been studying electron multiplication properties in a gas along a metal edge, or blade. Similar techniques have been developed previously by other groups. These concentrated on operation in the limited streamer mode [1], or the gas proportional mode [2] but were not developed specifically for synchrotron experiments. Our efforts have focussed on operation in the gas proportional mode, with emphasis on small electrode spacing to maximize count rate performance. Systematic studies are being carried out to optimize overall performance for synchrotron applications.

## II. BASIC STUDIES OF ELECTRON MULTIPLICATION ON A BLADE

### A. Experimental Setup

A schematic of the test detector is shown in fig.1. The anode is steel shim stock, whose thickness ( $t$ ) is 25 $\mu$ m (unless specified otherwise), sandwiched between two cathodes, separated by a distance,  $d$ , using two fiberglass spacers. The spacers are recessed below the edge of the blade by about 1.8 mm ( $h$ ) to prevent charge buildup. The usable length of the electrodes (into the diagram) is 6 cm. In this initial work we have used  $d=2.4$ mm (3/32 inch), which provides a relatively short path for positive ions, created in an avalanche, to travel from the anode to cathode, and provides a footprint of cathode induced charge that conveniently permits the use

<sup>1</sup>This work was supported by the U.S. Department of Energy under contract No. DE-AC02-98CH10886.

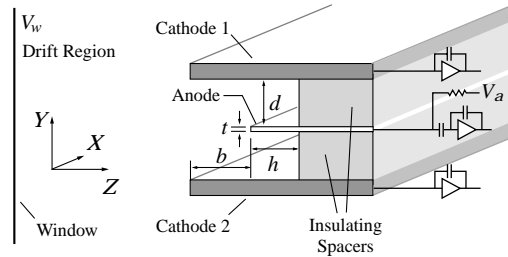


Figure 1. A schematic of the test chamber cross-section.

of an interpolating cathode technique for position sensing. The anode is connected through a preamplifier and shaping amplifier to a PHA. The two cathodes are individually connected to their own electronic channels, whose outputs are analyzed on a dual parameter PHA. Results reported are taken with 1 $\mu$ s delay line shaping amplifiers. The window to cathode distance was maintained at about 1cm, providing good detection efficiency for Cr K $\alpha$  x-rays (5.41 keV) in a gas mixture of Ar/20%CO<sub>2</sub>, with which all the measurements reported here were carried out. With the anode at positive bias (~2250V) and the cathodes at ground potential, a window voltage of  $V_w = -200$ V generated a drift-field that was sufficient to transport electrons to the anode without loss.

### B. Effect of Anode Recess

In this set of measurements, the cathodes were fabricated, simply, from 0.25mm thick steel shim stock. The recess,  $b$ , of the tip of the anode blade, with respect to the cathodes, influences the gas gain at a given anode voltage and the uniformity of the gain in the direction across the anode. It also affects the acceptance aperture in the drift region. The anode blade, remaining in the X-Z plane, was tilted such that  $b$  changed from zero at one end to about 5.5mm at the other end. This arrangement made it possible to study the dependence of anode gain on the magnitude of its recess, by simply scanning a collimated x-ray beam along the length of the blade. Fig. 2 shows the anode pulse height variation from

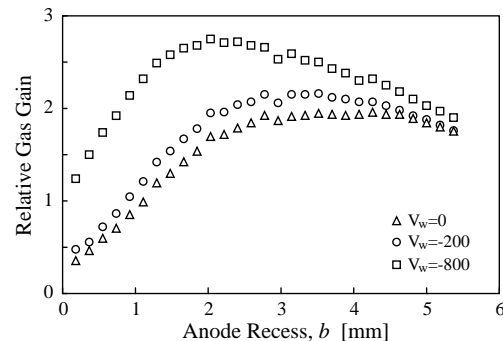


Figure 2. Gas gain variation as a function of anode recess. A collimated x-ray beam was centered over the anode blade.  $V_a = 2250$ V,  $V_w = -200$ V.

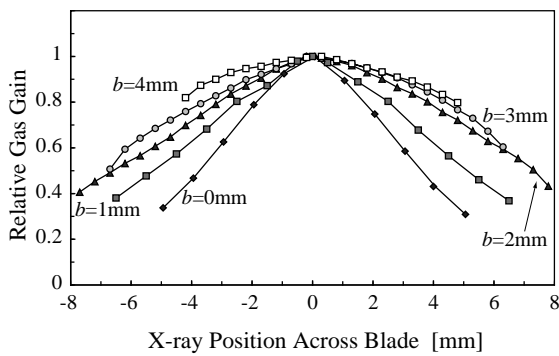


Figure 3. Gas gain variations from scans of a collimated x-ray beam along Y axis at different anode recesses.  $V_a = 2250\text{V}$ ,  $V_w = -200\text{V}$ . The maximum pulse height of each scan has been normalized. The origin of the Y axis is where the center of the blade is.

these measurements. When the recess is less than the anode-cathode spacing, the gas gain increases as the recess increases. However, this trend stops and even reverses itself as the recess becomes larger than the anode-cathode spacing. The reversal is more evident with the presence of a higher drift field. This behavior is believed to be the result of diminishing influence of the drift field on the anode tip as it recesses more deeply into the shielding of the cathodes.

Gain variation across the anode blade was investigated by scanning a collimated beam along the Y axis (fig.1). Fig. 3 demonstrates the influence of the anode recess on the gain uniformity across the blade, as well as the acceptance aperture in the drift region. A deeper recess improves the gain uniformity, but decreases the acceptance aperture. Many synchrotron experiments require an acceptance aperture of typically 10 mm in a one-dimensional detector. It is also desirable that the anode maintains a fairly uniform gain across this aperture. Since  $b = 4\text{mm}$  satisfies both of these criteria reasonably well, this value was selected to make further studies.

### C. Effect of Drift Field and Blade Thickness

Pulse height measurements across the blade were made, at the position where  $b = 4\text{mm}$ , as a function of drift field. The results, shown in fig.4, clearly illustrate that gain varia-

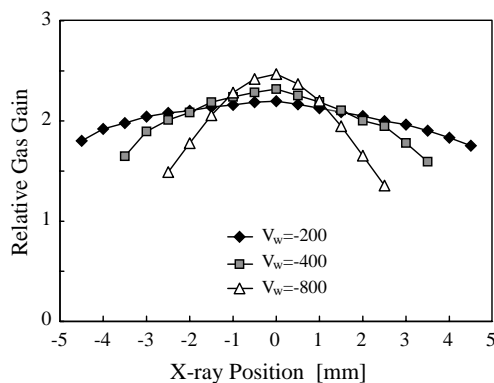


Figure 4. Gas gain variations from scans of a collimated x-ray beam along the Y axis across the blade under different window bias voltages. Anode bias voltage remains at 2250V.

tion increases as the magnitude of the drift field increases. Fig.5a and 5b show the calculated electron drift lines from the drift region ending on the anode for  $V_w = -200\text{V}$  and at a higher field ( $V_w = -800\text{V}$ ). In both cases the electric field varies from a strong, near cylindrical field directly above the tip of the anode to a considerably weaker field on each side of the anode. Therefore the gas gain of an electron varies according to its point of arrival at the anode surface. Specifically fig. 5 shows that at the lower drift field, field lines from a broad section of the drift region terminate, in a narrow angle, at the anode. In contrast, at the higher drift field, only lines from a restricted section of the drift region terminate at the anode, with a much wider angular spread, resulting in a larger gain variation. Fig.4 also shows that the acceptance aperture of the detector is reduced as the drift field increases, in accord with the field line pattern in fig.5. Further investigations are in progress to study the role of the blade thickness and shape of tip in gain uniformity.

The uniformity of gain along the length of the blade was measured with a constant anode recess,  $b=4\text{mm}$ , along the full 6cm length. A scan of the collimated x-ray beam revealed the gain was reasonably uniform, within  $\pm 10\%$ , over this length. The energy resolution is also quite good for a collimated x-ray beam, with a FWHM  $\sim 25\%$  for 5.4keV x-rays at 0.1pC anode charge level. An anode charge level of 2pC was achieved in this setup, which demonstrated its stability.

### D. Anode Avalanche Angular Localization

In gas proportional detectors using induced cathode charge for position encoding, it is important to understand the effect of anode avalanche angular localization [3]. 2-D histograms of the two cathode signals from uniform irradiation are shown in fig.6. Some interesting phenomena are revealed.

Clearly the induced charges on the two cathodes are not always equal. Instead of forming a narrow band along a  $45^\circ$  angle, the events form a wedge shape with a finite opening

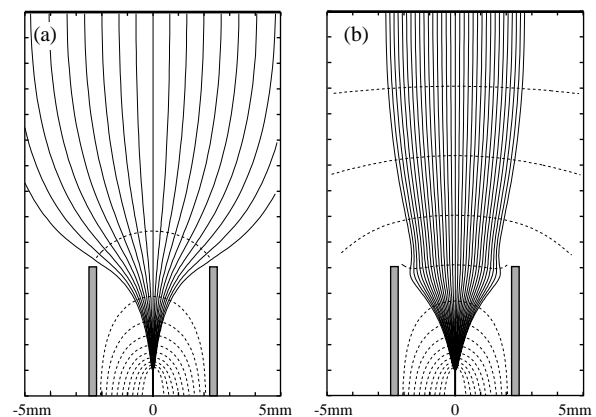


Figure 5. Computer simulated electric field lines and equipotential contours in the test setup with window bias voltage of (a) -200V and (b) -800V. Only those field lines that connect both the anode blade and the window are shown. Cathodes are grounded,  $V_a = 2250\text{V}$ .

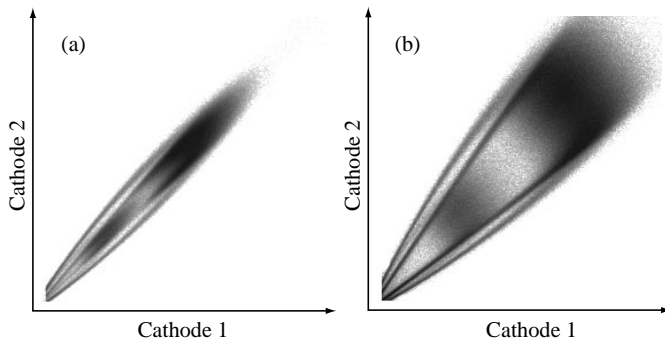


Figure 6. 2D histograms of the induced charge correlation on the two cathodes: (a) 25 $\mu\text{m}$  blade with  $V_w$  of -200V; (b) 76 $\mu\text{m}$  blade with  $V_w$  of -800V. The anode charge level was set at about 0.1pC for both measurements.  $b=4\text{mm}$ . Uniform irradiation over about 6mm length across the anode. Intensity scale is logarithmic.

angle, which reflects the degree of asymmetry in the two cathode induced charges. For this particular electrode geometry, the angle is dependent on the anode width, being significantly larger for the 76 $\mu\text{m}$  blade. Further measurements have shown that the opening angle reduces at smaller shaping time (since the positive ions are all closer to the anode) and is largely independent of anode charge level.

### E. Induced Charge Profile on the Cathode

A convenient way to extract avalanche position information from this electrode configuration is to use an interpolating technique to sample the induced cathode charge, as is common in various types of proportional wire chambers [4]. Using a printed circuit board, a test cathode was fabricated that consisted of a continuous plane of copper except for two sets of strips that run along and across the blade length; this replaced one of the metal shim cathodes. The induced cathode charge profiles across and along the blade direction were measured by sampling the charge on these two sets of strips. The charge distribution along the blade, shown in fig. 7, can be fitted closely to the empirical single parameter Gatti distribution [5]. The induced charge profile across the blade shows some level of asymmetry, at least in part because of asymmetry in the positive ion movement across the blade. These charge profiles provide the information required for designing position interpolating cathode structures with low differential non-linearity.

## III. DEVELOPMENT OF A CURVED DETECTOR

A 1-D position sensitive x-ray detector has been constructed with a blade anode for a large angle x-ray diffraction experiment at Brookhaven's National Synchrotron Light Source. In order to eliminate parallax errors at large diffraction angles, the anode blade and other electrodes are curved. Fig. 8 shows a photograph of all major parts in this detector's assembly. It covers an angle of 45°, has an arc length of about 20cm with a radius of curvature of 25cm. The blade is fabricated from a 25 $\mu\text{m}$  thick stainless steel sheet using electric discharge machining. The blade recess

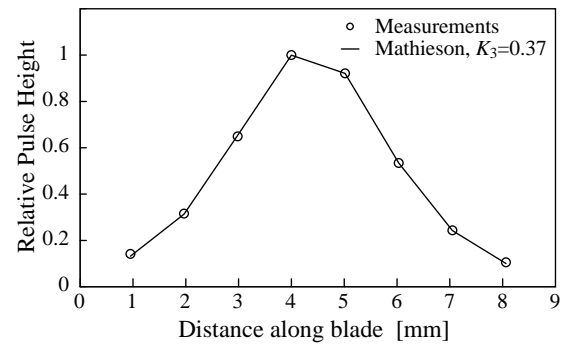


Figure 7. Induced charge profile along the blade as measured by a set of 1mm wide cathode strips.

and anode cathode spacing are set at 4mm and 2.4mm respectively, optimized values determined from the earlier studies. In addition, drift field defining electrodes are used to improve electron collection. The two cathodes are made of printed circuit boards, with 40 copper zigzag shaped strips [4] running radially on each cathode facing the anode blade. Corresponding facing cathode strips are electrically connected together as a single readout node (thus virtually all the cathode charge is utilized for position encoding). These readout nodes can be connected to either a conventional delay line readout system [6] or a newly developed digital centroid-finding system [7]. The delay line readout system has been used in many 1D and 2D MWPC based position sensitive x-ray detectors developed by our group. In the digital centroid-finding system, the signal from each node is first amplified by a preamp and a shaper, and then pro-

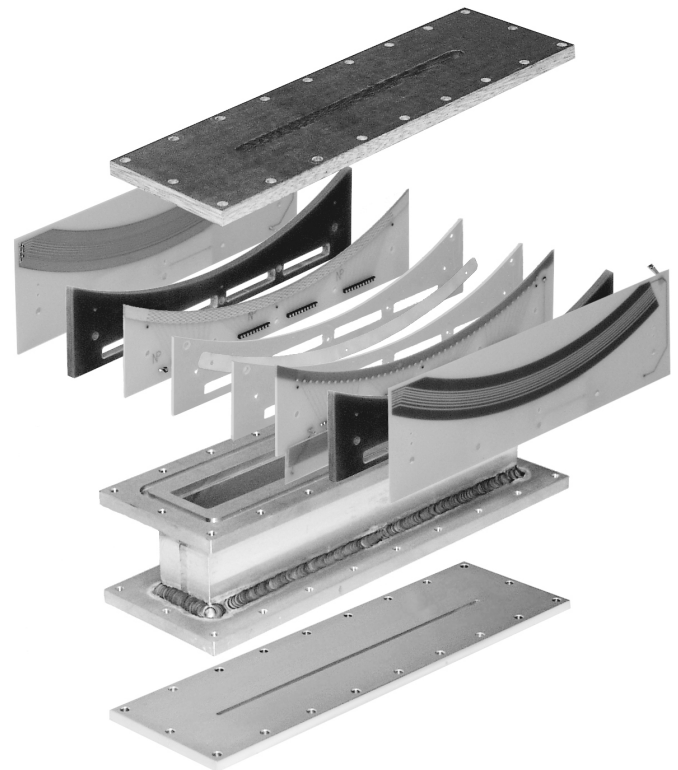


Figure 8. An exploded view of all major components in the curved detector.

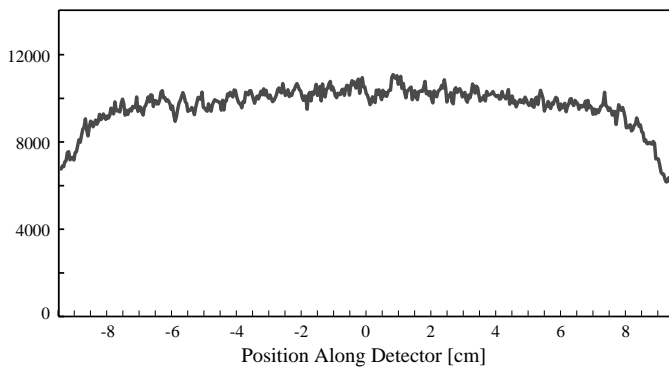


Figure 9. Detector's uniform irradiation response using a 1 $\mu$ s delay line readout. The fall-off at the ends of the detector is due to the x-ray source.

cessed by the centroid-finding module. Each module contains 16 input channels. A set of free running 20MHz ADCs digitizes every channel at 50ns intervals to an 8bit precision. An FPGA (Field Programmable Gate Array) chip monitors 16 input channels using a programmed logic to identify an x-ray event and transfer the three adjacent ADC channels that have the maximum pulse heights to a DSP (Digital Signal Processor). The DSP calculates the reconstructed position of the x-ray event using a prescribed algorithm and performs histogramming in its internal memory. The system is capable of decoding multiple simultaneous hits and providing a maximum sustained throughput of 2 MHz. A detailed description of this system is given in ref. 7.

Preliminary analysis of the detector has been performed using both the delay line readout system and the digital centroid-finding system. Results from the digital readout are described in ref. 7. Since the behavior of the delay line readout system is well understood, its results serve as a good reference to understand the behavior of the digital system.

Position linearity is measured from the detector's uniform irradiation response. As shown in fig. 9, the differential non-linearity is about 10%. Previous studies on the position response of a MWPC with zigzag cathode strips have shown that the location of the anode wires with respect to the zigzag apices is critical to the linearity of the readout system. The best result is obtained with the anode wire (or the center of gravity of the induced charge distribution) aligned between the zigzag apices. However, in the case of the blade, the induced cathode charge distribution is moving along the Z axis due to the movement of the positive ions. In addition, the induced charge distribution is not symmetrical in that direction. These complicate the design of the zigzag pattern. Nevertheless, further reduction in the non-linearity can be expected by optimizing the geometry of the zigzag cathode pattern.

The position resolution of the detector as a function of the anode charge is shown in fig. 10. Previous studies have shown that the ultimate limit on the position resolution under these conditions is about 100 $\mu$ m (FWHM) due to the range of the photoelectrons. The best result obtained so far with

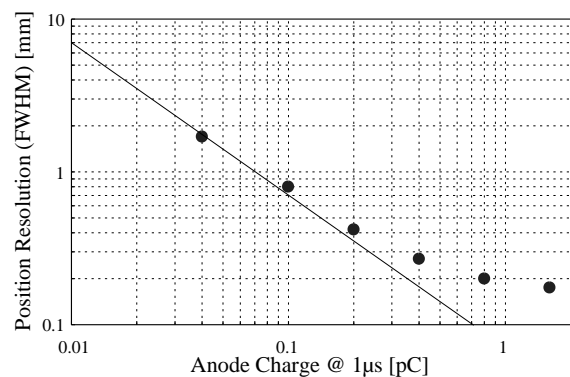


Figure 10. Position resolution as a function of anode charge level of the curved detector. (5.4 keV x-rays, Argon/20% CO<sub>2</sub> mixture, 1 $\mu$ s delay line readout)

the delay line readout is about 175 $\mu$ m at an anode charge level of 1.6 pC (1 $\mu$ s). Similar measurements with the digital centroid-finding system yielded about 140 $\mu$ m at 0.2 pC. Figure 10 indicates that the detector is not quite noise limited at large charge levels. It is possible that the spread of avalanche at large anode charge levels is more severe on the tip of the blade than on a cylindrical wire.

The present detector will be modified to include 64 readout nodes to improve the resolution and rate capabilities. A larger detector with a 120° angular coverage and 40cm arc length is also under construction.

#### IV. ACKNOWLEDGMENTS

The authors are grateful for the skillful assistance of E.F. Von Achen in preparing the detector assemblies.

#### V. REFERENCES

- [1] J. Ballou, V. Comparat and J. Pouxe, "The Blade Chamber: A Solution for Curved Gaseous Detectors," *Nucl. Instr. Meth.* 217 (1983) 213–216.
- [2] J.H. Duijn et al, "A Curved Razor-Blade Proportional Counter for X-ray Diffraction," *IEEE Trans. Nucl. Sci.* 33 (1986) 388–390.
- [3] G. Charpak and F. Sauli, "Multiwire proportional chambers and drift chambers," *Nucl. Instr. Meth.* 162 (1979) 405–428.
- [4] E. Mathieson and G.C. Smith, "Reduction in non-linearity in position-sensitive MWPCs," *IEEE Trans. Nucl. Sci.* NS-36 (1989) 305–310.
- [5] E. Mathieson and J.S. Gordon, "Cathode Charge Distribution in Multiwire Chambers, II. Approximate and empirical formulae," *Nucl. Instr. Meth.* 227 (1984) 277–282.
- [6] R.A. Boie et al, "High Resolution X-ray Gas Proportional Detectors with Delay Line Position Sensing for High Counting Rates," *Nucl. Instr. Meth.* 201 (1982) 93–115.
- [7] P.J. Pietraski et al., "Digital Centroid-Finding Electronics for High-Rate Detectors" submitted to these proceedings.